



**Faculty of Mechanical Engineering**

**STUDY OF BIOMECHANICAL PROPERTIES OF ARTICULAR  
CARTILAGE USING LOW-FIELD  
MAGNETIC RESONANCE IMAGING**

**Yew Wansin**

**Master of Science in Mechanical Engineering**

**2017**

**STUDY OF BIOMECHANICAL PROPERTIES OF ARTICULAR CARTILAGE  
USING LOW-FIELD MAGNETIC RESONANCE IMAGING**

**YEW WANSIN**

**A thesis submitted  
in fulfilment of the requirements for the degree of Master of Science  
in Mechanical Engineering**

**Faculty of Mechanical Engineering**

**UNIVERSITI TEKNIKAL MALAYSIA MELAKA**

**2017**

## DECLARATION

I declare that this thesis entitled “Study of Biomechanical Properties of Articular Cartilage using Low-Field Magnetic Resonance Imaging” is the result of my own research except as cited in the references. The thesis has not been accepted for any degree and is not concurrently submitted in candidature of any other degree.

Signature : .....

Name : Yew Wansin

Date : .....

## **APPROVAL**

I hereby declare that I have read this thesis and in my opinion, this thesis is sufficient in terms of scope and quality for the award of the Master of Science in Mechanical Engineering.

Signature : .....

Supervisor Name : Associate Prof. Dr. Mohd Juzaila Bin Abd Latif

Date : .....

## **DEDICATION**

With my deepest gratitude that I dedicate this thesis to my beloved parents and family for their endless love and support. This is also dedicated to my respectful supervisor for his mentorship throughout this study, examiners, lecturers and all my friends for their unwavering support over the years.

## ABSTRACT

Osteoarthritis (OA) is a major health issues among the population, causing pain in the human joints. It is well recognised that the OA is mainly caused by the degeneration of articular cartilage. The earliest stage of OA resulted in the alteration of the biomechanical properties of cartilage elastic modulus and permeability. Hence, the ability to detect the disease at its earliest stage is crucial for early intervention of the disease. MRI technique is widely used to assess the condition of the articular cartilage by examining the geometrical data. However, most of the diagnoses were performed at the progressive stage of osteoarthritis. Furthermore, most of the previous works and current clinical procedures were performed using high-field MRI which require significant purchase and maintenance costs. Therefore, this study aimed to investigate the potential application of low-field MRI image in order to examine the condition of articular cartilage. Cartilage specimens obtained from the humeral head of bovine were scanned using 0.18 T MRI. It was found that the gradient echo sequence of the low-field MRI was the most suitable sequence to image the cartilage. The images of cartilage were characterised based on the intensity of the greyscale. Creep indentation test was then conducted on the cartilage specimens and subsequently the indentation test was simulated using finite element method. The biomechanical properties of cartilage elastic modulus and permeability were characterised by integrating the experimental indentation test data and computational finite element model. The average elastic modulus was found to be  $0.93 \pm 0.72$  MPa while the permeability was  $0.58 \pm 0.31 \times 10^{-15} \text{m}^4/\text{Ns}$ . Correlation analyses were performed to examine the relationship between the greyscale of MRI image and biomechanical properties of elastic modulus and permeability of the cartilage. It was found that the cartilage greyscale was moderately correlated with cartilage biphasic elastic modulus ( $r= 0.513$ ) and higher correlation was observed with the permeability ( $r= 0.613$ ). Thus, present results indicate that the low-field MRI have the potential and provide promising insight to determine the condition of articular cartilage. It could be further develop to serve as an early intervention of OA disease.

## ABSTRAK

*Osteoarthritis dikenalpasti sebagai salah satu isu kesihatan yang menyebabkan kesakitan pada sendi manusia. Degenerasi tulang rawan artikular dikenalpasti sebagai punca utama osteoarthritis. Pada peringkat awal osteoarthritis, ciri-ciri biomekanikal elastik dan kebolehtelapan tulang rawan akan mengalami perubahan. Kajian mendalam mengenai tulang rawan telah banyak dijalankan semasa perubahan patologi pada tisu rawan. Oleh itu, keupayaan untuk mengesan osteoarthritis pada peringkat awal adalah penting untuk intervensi awal bagi rawatan penyakit ini. Kaedah pengimbas pengimejan resonans magnetik digunakan secara meluas untuk mengkaji keadaan tulang rawan artikular melalui pemeriksaan data geometri. Walau bagaimanapun, diagnosis ini biasa dijalankan pada peringkat perkembangan osteoarthritis. Kebanyakan kajian lanjutan terdahulu dan prosedur klinikal semasa telah dijalankan dengan mengaplikasikan medan pengimejan resonans magnetik berkekuatan tinggi yang memerlukan kos pembelian dan penyelenggaraan yang tinggi. Oleh itu, kajian ini bertujuan untuk mengkaji potensi pengimejan resonans magnetik berkekuatan rendah dalam pemeriksaan keadaan tulang rawan. Tulang rawan daripada humerus sendi bahu lembu telah digunakan untuk pengimejan dengan mengaplikasikan medan pengimejan resonans magnetik yang berkekuatan serendah 0.18 T. Di dalam kajian ini, didapati urutan gema kecerunan adalah urutan yang paling sesuai dalam pengimejan resonans magnetik berkekuatan rendah untuk mengkaji tulang rawan. Imej tulang rawan ini kemudian dicirikan mengikut keamatan skala kelabu. Ujian lekukan dijalankan untuk mendapatkan data daripada eksperimen dan model unsur tak terhingga telah dibangunkan daripada pengukuran geometri tulang rawan. Kajian mengkaji ciri-ciri biomekanikal tulang rawan dilakukan dengan mengintegrasikan data eksperimen ujian lekukan dan pengkomputeran unsur tak terhingga. Nilai purata elastik modulus tulang rawan adalah  $0.93 \pm 0.72$  MPa manakala purata untuk kebolehtelapan adalah  $0.58 \pm 0.31 \times 10^{-15} \text{m}^4/\text{Ns}$ . Analisis korelasi telah dikaji untuk mengenalpasti hubungan antara skala kelabu dan sifat biomekanikal modulus elastik dan kebolehtelapan tulang rawan. Berdasarkan hasil kajian, skala kelabu tulang rawan menunjukkan hubungan sederhana dengan modulus elastik ( $r=0.513$ ) dan hubungan yang lebih tinggi diperhatikan pada kebolehtelapan ( $r=0.613$ ). Hasil dari kajian ini menunjukkan pengimejan resonans magnetik yang berkekuatan rendah berpotensi untuk menentukan keadaan tulang rawan artikular. Pendekatan ini boleh dikaji secara mendalam bagi memberi panduan kepada intervensi rawatan yang awal dalam bidang penyelidikan penyakit osteoarthritis.*

## ACKNOWLEDGEMENTS

First and foremost, I would like to take this opportunity to offer my sincerest acknowledgement to my supervisor, Associate Professor Dr Mohd Juzaila Bin Abd Latif from the Faculty of Mechanical Engineering Universiti Teknikal Malaysia Melaka (UTeM) for his essential supervision, optimistic inspiration, invaluable advice, and constructive guidance from the beginning of the study towards the completion of my research.

Besides that, heartfelt gratitude goes to Dr Norhashimah Binti Mohd Saad from the Faculty of Electronic and Computer Engineering Universiti Teknikal Malaysia Melaka (UTeM), co-supervisor of this project for her kind supervision, assistance, and enlightening advices regarding on my research. She helped me a lot in my early stage of the project.

Special thanks to Universiti Teknikal Malaysia Melaka (UTeM) and the financial support from Ministry of Education Malaysia (MOE) for the MyMaster sponsorship throughout this project. I would like to give an appreciation to the Ministry of Science, Technology and Innovation (MOSTI) for the Science Fund financial support of the research project no. 06-01-14-SF0109 L00020.

With a great pleasure, I would also like to express my deepest gratitude and special appreciation to all my lecturers, fellow friends, and lab members from Lab Advanced Digital Signal Processing (ADSP) for their encouragement, willingness support, and constructive advice through my study.

I would like to offer my thanks and love to my beloved family who provided me with continuous prayers, patience, and moral support for me.

Lastly, thank you to everyone who had been directly or indirectly involved in the crucial parts of realisation of my master study.



---

## TABLE OF CONTENTS

	PAGE
<b>DECLARATION</b>	
<b>APPROVAL</b>	
<b>DEDICATION</b>	
<b>ABSTRACT</b>	<b>i</b>
<b>ABSTRAK</b>	<b>ii</b>
<b>ACKNOWLEDGEMENTS</b>	<b>iii</b>
<b>TABLE OF CONTENTS</b>	<b>iv</b>
<b>LIST OF TABLES</b>	<b>vii</b>
<b>LIST OF FIGURES</b>	<b>ix</b>
<b>LIST OF APPENDICES</b>	<b>xii</b>
<b>LIST OF ABBREVIATIONS</b>	<b>xiii</b>
<b>LIST OF SYMBOLS</b>	<b>xv</b>
<b>LIST OF PUBLICATION</b>	<b>xvi</b>
<b>CHAPTER</b>	
<b>1. INTRODUCTION</b>	<b>1</b>
1.1 Project Background	1
1.2 Problem Statement	4
1.3 Objectives	5
1.4 Scope	5
1.5 Significance of Study	6
1.6 Outline of Thesis	6
<b>2. LITERATURE REVIEW</b>	<b>8</b>
2.1 Synovial Joint	8
2.1.1 Anatomy of Synovial Joint	8
2.1.2 Types of Synovial Joint	9
2.2 Osteoarthritis	11
2.2.1 Causes	12
2.2.2 Diagnosis	14

2.2.3	Treatment	19
2.3	Articular Cartilage	20
2.3.1	Composition	21
2.3.2	Structure	24
2.3.3	Properties Characterisation	26
2.3.3.1	Specimen Preparation	26
2.3.3.2	Thickness	28
2.3.3.3	Biomechanical Properties	30
2.3.3.4	Computational Method	34
2.4	Magnetic Resonance Imaging	36
2.4.1	Physical Basic of MRI	38
2.4.2	Magnetic Field Strength	39
2.4.3	MRI Sequences	43
2.4.4	Greyscale Intensity	44
2.5	Low-field MRI Studies of Articular Cartilage	45
2.6	Animal Model	48
2.7	Summary	51
<b>3.</b>	<b>METHODOLOGY</b>	<b>53</b>
3.1	Material and Specimen Preparation	55
3.1.1	Phosphate Buffered Saline	55
3.1.2	Specimen Preparation	55
3.1.3	Frozen Specimen Preparation	57
3.2	Magnetic Resonance Imaging	57
3.2.1	MRI Image Acquisition for Cartilage	59
3.2.2	MRI Image Processing	60
3.2.3	Characterisation of the MRI Image	60
3.3	Experimental method	61
3.3.1	Indentation Apparatus	62
3.3.2	Calibration Procedure	63
3.3.3	Creep Indentation Test	64
3.4	Cartilage Thickness Measurement	66

3.5	Measurement of Cartilage Curvature	68
3.6	Computational Method	69
3.6.1	Verification of Finite Element Model	70
3.6.2	Development of Finite Element Model	73
3.6.3	Mesh Sensitivity Analysis	75
3.7	Characterisation of Cartilage Biomechanical Properties	77
3.8	Statistically Analysis	79
3.9	Summary	80
<b>4.</b>	<b>RESULTS AND DISCUSSION</b>	<b>81</b>
4.1	Selection of MRI Sequence	81
4.2	Characterisation of Cartilage Greyscale	83
4.3	Cartilage Thickness Measurement	87
4.4	Biomechanical Properties of Cartilage	88
4.5	Correlation of Cartilage Greyscale and Biomechanical Properties	91
4.6	The Effects of Cartilage Storage on Cartilage Biomechanical Properties	94
4.7	Overall Discussion	98
<b>5.</b>	<b>CONCLUSION AND RECOMMENDATION</b>	<b>99</b>
5.1	Conclusion	99
5.2	Recommendation	100
	<b>REFERENCES</b>	<b>102</b>
	<b>APPENDIX A</b>	<b>117</b>
	<b>APPENDIX B</b>	<b>118</b>
	<b>APPENDIX C</b>	<b>120</b>
	<b>APPENDIX D</b>	<b>129</b>
	<b>APPENDIX E</b>	<b>132</b>
	<b>APPENDIX F</b>	<b>134</b>

## LIST OF TABLES

<b>TABLE</b>	<b>TITLE</b>	<b>PAGE</b>
2.1	Causes of OA	13
2.2	List of osteoarthritis features	15
2.3	Imaging modalities and morphological features of articular cartilage	16
2.4	Types of collagen and their function	23
2.5	Thickness of cartilage measured using indentation test method	29
2.6	Biphasic biomechanical properties of articular cartilage in human synovial joints	33
2.7	Biphasic biomechanical properties of articular cartilage in animal synovial joints	33
2.8	Material constitutive model of the articular cartilage	36
2.9	Cartilage studies conducted using various magnetic field strength of MRI	40
2.10	Cartilage studies using low-field MRI	47
2.11	Animal models used in previous studies	50
3.1	The acquisition parameters of the MRI sequences	60
3.2	Cartilage material properties of articular cartilage for FE verification model	71
3.3	Material properties for the finite element model	74
4.1	MRI images of articular cartilage using various sequences	82

4.2	Thickness of the bovine cartilage	87
4.3	Elastic modulus of bovine articular cartilage	89
4.4	Permeability of bovine articular cartilage	90

## LIST OF FIGURES

FIGURE	TITLE	PAGE
1.1	MRI image (a) 1.5 T MRI and (b) 0.2 T MRI show equally diagnostic performance on the meniscal injuries.	3
2.1	Structure of synovial joint in knee.	9
2.2	Types of synovial joint.	10
2.3	Normal cartilage (left) and degenerated cartilage (right) between the femur and tibia.	12
2.4	Corresponding sagittal, axial, and coronal images using (a) clinical CT scan and (b) MRI.	18
2.5	Left, full thickness chondral defect. Right, osteochondral autograft mosaicplasty with two plugs.	20
2.6	Diagram of proteoglycan aggregate and aggregan molecule.	24
2.7	The structural of articular cartilage from the superficial zone to the deep zone.	25
2.8	Mechanical testing configurations (a) Unconfined compression (b) Confined compression (c) Indentation test.	31
2.9	Comparison of the appearance of the articular cartilage of the distal interphalangeal joint of horse in sagittal view obtained by (a) the high-field; (b) the low-field; (c) the cartilage appears as a single layer axially.	42
2.10	Example of DICOM image that represents by different pixel values.	44
3.1	Flowchart of the overall methodology.	54
3.2	Specimen preparation process (a) Bovine humeral head marked equally into four sections (b) Specimen cutting process using electric saw (c) The region of interest (ROI) of cartilage specimen.	56
3.3	Cartilage specimen covered with PBS soaked tissue.	57

3.4	The C-scan MRI system.	58
3.5	Specimen placed in the receiving coil.	59
3.6	(a) MRI image of the articular cartilage from gradient echo sequence (b) Close view of the MRI image and cropped image.	61
3.7	Schematic diagram of indentation test rig.	62
3.8	Procedure of the calibration test (a) Set-up of the calibration test (b) Different height of stainless steel gauge blocks.	63
3.9	Graph represents the measurement taken in the load calibration.	64
3.10	Apparatus for indentation test (a) Components of the test rig (b) Specimen holder (c) 4mm diameter of the spherical indenter (d) Close view on the indented specimen.	65
3.11	Apparatus for indentation thickness test. (a) Close-view on the thickness test (b) Needle indenter.	67
3.12	Response of load and displacement transducers for cartilage thickness measurement.	68
3.13	Measurement of the cartilage curvature using profile projector.	69
3.14	Axisymmetric FE model for contact dependent flow of a flat cartilage.	71
3.15	Contact pressure distribution on the cartilage surface for (a) Stress-relaxation (b) Creep deformation at 2 seconds and 1000 seconds.	72
3.16	Pore pressure distribution on the cartilage surface for (a) 2 seconds (b) 1000 seconds.	72
3.17	Axisymmetric FE model of the cartilage specimen.	73
3.18	Examples of finite element mesh for mesh sensitivity analysis. (a) 320 elements (b) 2000 elements.	75
3.19	Contact pressure versus deformation of cartilage at 1000 seconds.	76
3.20	Contact pressure distribution of the cartilage at (a) 2 seconds (b) 1000 seconds.	77
3.21	Cartilage deformation curve.	79

4.1	MRI image of cartilage.	84
4.2	Cartilage greyscale of the superficial zone and deep zone of the cartilage.	85
4.3	Cartilage water content along the depth of the articular cartilage.	86
4.4	Average cartilage thickness of bovine humeral head.	88
4.5	Cartilage biphasic elastic modulus characterised from different sites of bovine specimens.	89
4.6	Cartilage biphasic permeability characterised from different sites of bovine specimens.	90
4.7	Linear Pearson correlation between the greyscale and elastic modulus of the cartilage.	92
4.8	Linear Pearson correlation between the greyscale and permeability of the cartilage.	92
4.9	Comparison of the MRI greyscale for fresh and frozen specimens.	95
4.10	Total MRI greyscale for fresh and frozen specimens.	96
4.11	Comparison of the average elastic modulus for fresh and frozen cartilage specimens.	96
4.12	Comparison of the average permeability for fresh and frozen cartilage specimens.	97



## LIST OF APPENDICES

APPENDIX	TITLE	PAGE
A	Matlab Script	117
B	MRI Technical Specifications	118
C	Creep Indentation Test	120
D	Thickness Test	129
E	Biomechanical Properties of Cartilage	132
F	Publication	134

## LIST OF ABBREVIATIONS

CAX4	–	Four-node bilinear element
CAX4P	–	Four-node bilinear displacement and pore pressure
CAX4RP	–	Four-node bilinear displacement and pore pressure element, reduce integration
CT	–	Computed tomography
DAQ	–	Data acquisition
DICOM	–	Digital imaging and communications in medicine
ECM	–	Extracellular matrix
FE	–	Finite element
GRE	–	Gradient echo
LL	–	Lateral left
LR	–	Lateral right
LVDT	–	Linear variable differential transformer
ML	–	Medial left
MR	–	Medial right
MRI	–	Magnetic resonance imaging
OA	–	Osteoarthritis
PBS	–	Phosphate buffered saline
ROI	–	Region of interest
SE	–	Spin echo
T3D	–	Turbo 3D

US	–	Ultrasound
WHO	–	World Health Organisation
1D	–	One-dimensional
2D	–	Two-dimensional
3D	–	Three-dimensional

## LIST OF SYMBOLS

$E$	–	Elastic modulus
$k$	–	Permeability
$\nu$	–	Poisson's ratio
$e$	–	Void ratio
T	–	Tesla
$r$	–	Correlation coefficient
°C	–	Celsius

## LIST OF PUBLICATION

- 1) Yew, W.S., Latif, M.J.A., Saad, N.H M., 2016. Characterization of Grayscale of MRI Images for Articular Cartilage, *Proceedings of Mechanical Engineering Research Day 2016*, pp. 143-144.
  
- 2) Yew, W.S., Latif, M.J.A., Saad, N.H M., Alhabshi, S.M.I., Mahmud, J., Kadir, M.R.A., 2017. Characterization of Articular Cartilage using Low-Field Magnetic Resonance Imaging Image, *Journal of Medical Imaging and Health Informatics*, volume 7, pp. 1-4. (ISI Journal Accepted).

## CHAPTER 1

### INTRODUCTION

#### 1.1 Project Background

Osteoarthritis (OA) is one of the degenerative arthritis joint disorder that is most prevalent in knee, hips, and spine and it is one of the major health issue. It causes joint pain and stiffness. OA patients will have limitations in movement, cannot perform their major daily activities, and require help with care. It is estimated that 5.93% of the total population in Malaysia will develop osteoarthritis (Raj et al., 2016, 2014). The World Health Organisation (WHO) estimates that 9.6% of men and 18 % of women aged above 60 years old have affected by symptomatic OA (United Nations, 2015; Thysen et al., 2015; Leung et al., 2013). As the ageing population of the developed country increases, the prevalence of OA is expected to accelerate from 2015 to 2050 due to the proportion of the world's populations over 60 years has increased substantially.

OA is mainly caused by the deterioration of articular cartilage and affected the biomechanical properties of the articular cartilage at the early stage (Hani et al., 2015; Szarko et al., 2010; Knecht et al., 2006). Deterioration of cartilage is caused by wear or tear in the joint. It is most likely associated with ageing where it reduces the hydration of cartilage and affected the articular cartilage that have been continually stressed throughout the years to become thin and thus lead to the disease. Damaged cartilage become porous and high in permeability and leads to the decreased of modulus of elasticity and reduction in load bearing capacity (Grenier et al., 2014; Bhosale and Richardson, 2008). Due to the limited regenerative capacity of the articular cartilage, cartilage tissues repair remains a challenging task. Consequently, preventive strategies are yet to be identified to treat the

disease since the current prescriptions to modify or decelerate the disease are limited. In addition, non-surgical treatments for OA have limited efficacy partly due to the late detection of the structural deterioration of the disease (Favero et al., 2015). Therefore, in the final stage of the disease, most of the severe patient will undergo joint replacement surgery (Wang et al., 2012). Thus, the ability to diagnose the disease at its earliest stage is crucial because the treatment often depends on the early detection in the symptomatic OA disease.

Therefore, early detection of OA had caused great interest to researchers, radiologists, and orthopaedists. Nowadays, more than one measurement element of articular cartilage changes is needed to enhance the ability of the early symptoms of osteoarthritis. These include the alteration of cartilage composition components such as water content and proteoglycan content in cartilage and further examination on cartilage morphological components such as thickness and volume using imaging modalities (Hani et al., 2015; Liess et al., 2002).

Articular cartilage is only a few millimetres thick and possesses an irregular shape that make the detection of the minor changes in the early degeneration of the disease more challenging (Hani et al., 2015). Due to this, articular cartilage does not heal by itself under biological situation (Bergmann et al., 2013). The current gold standard for the early identification to assess the articular cartilage and diagnose the evolution of OA is based on medical imaging modalities such as computed tomography (CT) scan, X-ray, arthroscopy, ultrasound (US) and magnetic resonance imaging (MRI).

In recent decades, MRI has become the significant non-invasive imaging modality to examine the joint as a measure of the OA disease and assess the pathologic changes in bone and tissues especially articular cartilage (Fornari et al., 2015; Nissi et al., 2004). MRI is widely used to detect the osteoarthritis feature because it produces a high sensitivity of

contrast image in detecting intra-articular structures compare to others imaging modalities (Fornari et al., 2015; Kumar et al., 2011; Blumenkrantz and Majumdar, 2007; Liess et al., 2002). Research results had indicated that MRI is the most promising imaging modality because MRI enables quantitative assessment to measure volume and thickness of cartilage and semiquantitative assessment to examine the composition of (Hani et al., 2015; Wang et al., 2012). High-field MRI was normally used in previous studies to determine the cartilage biomechanical properties based on the quantitative information from MRI images (Nissi et al., 2007; Nieminen et al., 2004; Wayne et al., 2003; Liess et al., 2002). Previous studies have reported that the diagnostic performance between high-field (1.5 T) and low-field (0.2 T) MRI showed equally well on the knee joint (Cotten et al., 2000). Figure 1.1 shows the images on the knee meniscal injuries appearance obtained from both high and low-field MRI. Therefore, in the present work, the aim is to investigate the potential application of low-field MRI image in examining the condition of cartilage as early intervention of OA disease.

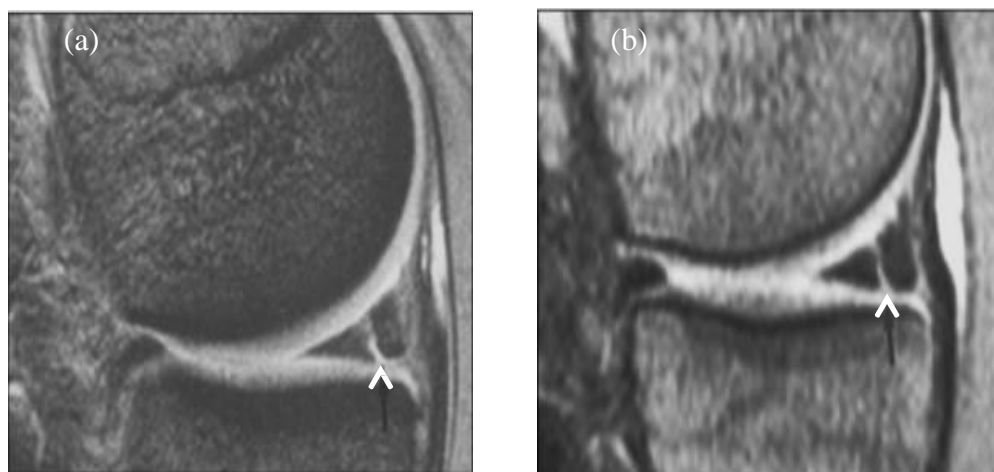


Figure 1. 1 MRI images (a) 1.5 T MRI and (b) 0.2 T MRI show equally diagnostic performance on the meniscal injuries (arrow). Adapted from Cotten et al., 2010